Surface & Coatings Technology 355 (2018) 16–21

Contents lists available at ScienceDirect

Surface & Coatings Technology

journal homepage: www.elsevier.com/locate/surfcoat

Depth profiles of aggregate centers and nanodefects in LiF crystals irradiated with 34 MeV ^{84}Kr, 56 MeV ^{40}Ar and 12 MeV ^{12}C ions

A. Dauletbekova[a,*], V. Skuratov[b,c,d], N. Kirilkin[b], I. Manika[e], J. Maniks[e], R. Zabels[e], A. Akilbekov[a], A. Volkov[b], M. Baizhumanov[f], M. Zdorovets[g,h], A. Seitbayev[g]

[a] L.N. Gumilyov Eurasian National University, Astana, Kazakhstan
[b] FLNR, JINR, Dubna, Russia
[c] National Research Nuclear University MEPhI, Moscow, Russia
[d] Dubna State University, Dubna, Russia
[e] Institute of Solid State Physics University of Latvia, Riga, Latvia
[f] Shakarim University Semey, Semey, Kazakhstan
[g] Institute of Nuclear Physics, Astana, Kazakhstan,
[h] Ural Federal University, Yekaterinburg, Russia

ARTICLE INFO

Keywords:
LiF crystals
Ion irradiation
Damage depth profiles
F_2 and F_3^+ centers
Photoluminescence
Dislocations
Hardening

ABSTRACT

Depth profiles of nanohardness and photoluminescence of F_2 and F_3^+ centers in LiF crystals irradiated with 12 MeV ^{12}C, 56 MeV ^{40}Ar and 34 MeV ^{84}Kr ions at fluences 10^{10}–10^{15} ions/cm^2 have been studied using laser scanning confocal microscopy, dislocation etching and nanoindentation techniques. The room temperature irradiation experiments were performed at DC-60 cyclotron (Astana, Kazakhstan). It was found that the luminescence intensity profiles of aggregate color centers at low ion fluences correlate with electronic stopping profiles. The maximum intensity of aggregate center luminescence is observed at fluence around 10^{13} ions/cm^2 and rapidly decreases with further increase of fluence. At the highest ion fluences, the luminescence signal is registered in the end-of-range area only. The depth profiles of nanohardness and chemical etching have shown remarkable ion-induced formation of dislocations and increase of hardness which in the major part of the ion range correlate with the depth profile of electronic energy loss. An exception is the end-of-range region where strong contribution of nuclear energy loss to hardening at high fluences is observed.

1. Introduction

Swift ion beams offer great opportunities for processing of solids and can be used to modify their structure, electronic, optical, mechanical and other properties.

Remarkable modification effects in LiF crystals are observed under conditions of high-fluence irradiation ensuring overlapping of ion tracks and formation of complex color centers, defect aggregates and extended defects, surface and bulk nanostructures [1–5]. Among complex color centers, F_2 and F_3^+ aggregate centers are found to be dominating in LiF irradiated with swift heavy ions at high fluence and flux [2], while ion-induced prismatic dislocation loops are revealed as the main extended defects formed at room temperature irradiation [5]. The knowledge and understanding of complex phenomena of the evolution of structure at the aggregation stage are of great importance for the development of technological applications of LiF (color center lasers, dosimetry, *etc.*). New possibilities have been offered by investigations of damage on profile surfaces along the ion trajectory. It provides information on peculiarities of damage at varying energy loss and varying contribution of electronic excitation and elastic collision (nuclear) mechanisms [6–8].

In the present work, depth profiles of complex color centers and dislocations in LiF crystals irradiated with ^{40}Ar, ^{84}Kr and ^{12}C ions at different fluences have been compared. The behavior of complex color centers (F_2 and F_3^+) along the ion path has been characterized by means of luminescence spectroscopy [7,8]. The evolution of nanodefects on profile surfaces has been investigated by chemical etching and instrumented nanoindentation which is a technique sensitive to dislocations and other extended defects. The attention has been focused on peculiarities of damage and property modifications in the end-of-range region where the dominant damage mechanism changes from the electronic excitations to the mechanism of elastic collisions (nuclear loss).

* Corresponding author.
E-mail address: alma_dauletbek@mail.ru (A. Dauletbekova).

https://doi.org/10.1016/j.surfcoat.2018.03.096
Received 27 October 2017; Received in revised form 5 March 2018; Accepted 12 March 2018
Available online 10 April 2018

2. Materials and methods

High quality LiF crystals grown from the melt in an inert atmosphere were used for the experiments. LiF platelets of 10 × 10 mm^2 and thickness of about 1 mm, cleaved from a single-crystal block, were irradiated at the cyclotron DC-60 (Astana, Kazakhstan) with 33.6 MeV ^{84}Kr, 56 MeV ^{40}Ar and 11.8 MeV ^{12}C ions. The thickness of the samples for all irradiations was substantially larger than the ion range (R) in LiF. The irradiations were performed at room temperature at fluences from 10^{10} to 10^{15} ions/cm^2. The ion beam current density was 10 nA/cm^2, which is low enough to avoid the target heating effects. The ion range and energy loss were calculated by SRIM 2013 code.

The LCSM NTEGRA Spectra confocal microscope was used to obtain depth resolved photoluminescence spectra of F_2 and F_3^+ color centers. For the source of excitation a laser with a wavelength of 473 nm was utilized. To prevent a damage of LiF samples a continuously variable ND filter with the attenuation range of 1–0.001 was set at minimum value to limit the output power of the laser source. The XYZ piezo stage of the microscope allowed scanning area of up to 100 × 100 μm in X-Y plane and up to 7 μm in Z direction with the minimum step of 0.01 μm. Spatial resolution for X-Y plane was measured with a regular Si calibration grating TGS-1 with a square profile and was determined to be approximately 0.3 μm. Each specimen of irradiated crystals was mounted on the XYZ stage with the ion penetration direction parallel to X axis and was scanned along the ion range with a step of 0.33 μm. The scanning was performed in Y axis with a step of 1 μm as well and subsequently the results were averaged.

Nanoindentation was performed by an instrumented indentation unit G200 (Agilent) in ambient air at room temperature using a Berkovich diamond tip. The area function of the indenter tip was calibrated using a silica reference sample. A basic nanoindentation technique with an indenter penetration depth of 150 nm at the strain rate 0.05 s^{-1} was used. Indentation tests were performed on samples prepared by cleaving of irradiated crystal normal to irradiated surface using conventional manual cleaving technique. Irradiated LiF cystals similar to unirradiated ones exhibit {100} type cleavage planes. The values of hardness (H) at nanoindentation tests were obtained using the Oliver–Pharr method [9]. The hardening effect (relative increase of hardness) was calculated as $(H-H_0)/H_0$ (%) where H_0 denotes the hardness of a virgin crystal, which at the selected 150 nm depth was H_0 = 1.5 GPa. The distance of indentation imprint from the irradiated surface served as the depth parameter and was measured by means of optical microscopy.

The dislocation structure in irradiated LiF samples was revealed by a short-time (1–2 s) selective chemical etching in a saturated aqueous $FeCl_3$ solution and by a subsequent imaging by atomic force microscope CPII (Veeco) in the tapping-mode.

3. Results

3.1. Depth-resolved photoluminescence of F_2 and F_3^+ color centers

For all investigated ions, their electronic energy loss in LiF does not exceed the 10 keV/nm threshold for the formation of a track core (Fig. 1), therefore the tracks are composed of a trail of simple and aggregated color centers together with the complementary hole centers [1]. F_2 and F_3^+ color centers, being very close in the optical absorption spectra (445 nm band), can be exactly distinguished by luminescence measurements [7,8]. The photoluminescence emission spectrum exhibits two peaks at about 670 nm (related to F_2) and 530 nm (related to F_3^+). As an example, the wavelength dependence of the normalized luminescence intensity for LiF irradiated with 33.6 MeV ^{84}Kr and 11.8 MeV ^{12}C ions at identical fluence is shown in Fig. 2.

The obtained depth profiles of the luminescence intensity related to F_2 and F_3^+ centers for all investigated ions are provided in Fig. 3. The maximum depth from which the luminescence signal is observed nearly

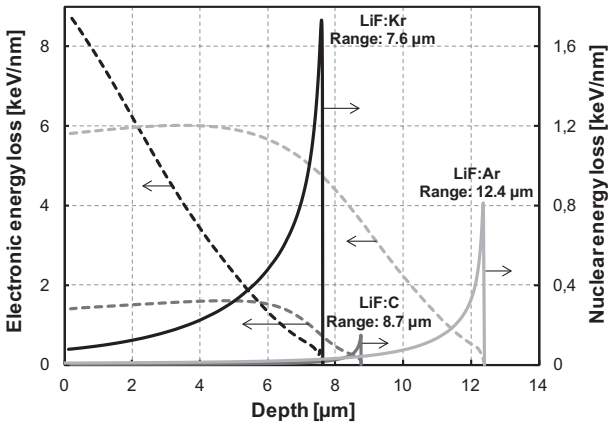

Fig. 1. Electronic (dashed line) and nuclear energy loss (solid line) of ^{84}Kr, ^{40}Ar and ^{12}C ions in LiF, calculated by SRIM.

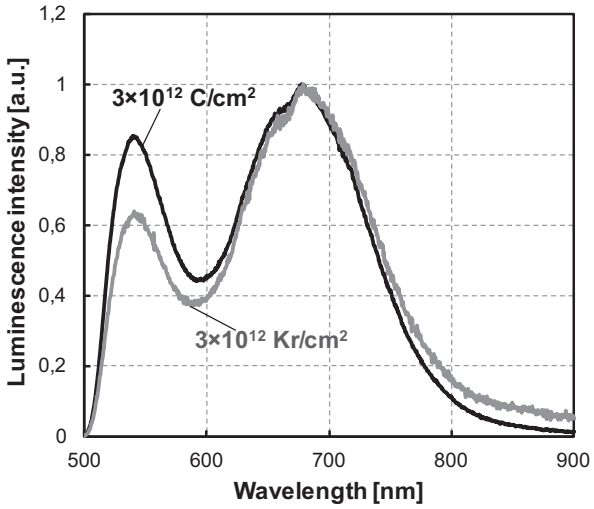

Fig. 2. The wavelength dependence of normalized luminescence intensity of F_3^+ (530 nm) and F_2 (670 nm) centers for LiF irradiated with 33.6 MeV ^{84}Kr and 11.8 MeV ^{12}C ions at fluence of 3 × 10^{12} ions/cm^2. Excitation source: 473 nm laser.

coincides with the ion range calculated by SRIM code and with the depth of damaged zone revealed by chemical etching.

The luminescence signal at comparatively low fluences, when mainly individual ion tracks are formed, gradually increases with the fluence and correlates with the depth profiles of electronic stopping power (Fig. 3). As known, concentration of the F-type color centers in lithium fluoride is determined by the energy deposited in the electron subsystem. Consequently, at low ion fluences in our investigated ion energy range the emission related to F_3^+ and F_2 color centers is detected near the surface, where the electronic stopping power has a maximum. Therefore, the luminescence yield continues to increase in any point of the irradiated layer until the absorbed dose will reach a level, when the non-radiative decay of the excited states in color centers will dominate over the radiative transitions. At higher fluences, when ion tracks overlap, luminescence signal shifts to the end-of-range region. The main peculiarity is the quenching of the luminescence intensity which starts at high fluences (around 10^{13} ions/cm^2) when ion tracks strongly overlap (Fig. 3a–d). In the case of lighter C ions, the critical concentration of defects required for the quenching of luminescence of F_2 centers is reached already at fluence of 3 × 10^{14} ions/cm^2 (Fig. 3f) while not yet for F_3^+ centers (Fig. 3e).

The photoluminescence quenching under high-fluence irradiation with high-energy ions is observed in numerous studies [8,10] and

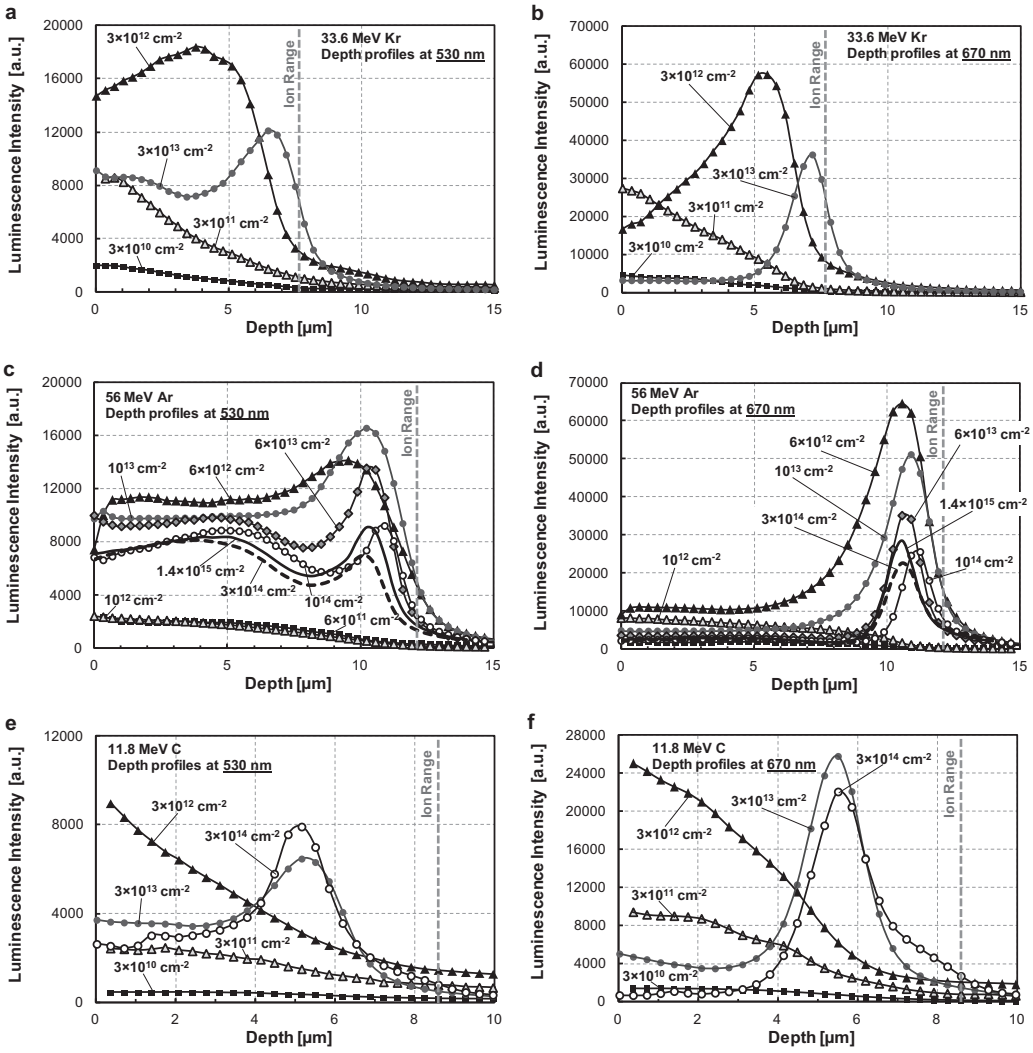

Fig. 3. Depth profiles of the luminescence intensity at 530 nm and 670 nm for samples irradiated with ^{84}Kr (a, b), ^{40}Ar (c, d) and ^{12}C (e, f) ions at different fluences. The end of the range is marked with a dashed line.

different explanations of this effect are offered. However, its mechanism is not fully understood. The increase of the concentration of aggregate color centers could give rise of non-radiative processes (concentration quenching) originated by an energy transfer between aggregate centers [11]. In [12] the quenching of photoluminescence at high concentration of aggregate centers is related to appearance of mechanical stress, suppressing the radiative decay of excited states. It should be noted that dislocations are a significant source of stress [13]. Therefore we consider the increase of the density of ion-induced dislocations (see Section 3.2) as one of possible factors facilitating the luminescence quenching.

3.2. Depth profiles of ion-induced hardening and dislocation structure

The depth profiles of hardness and energy loss for LiF samples irradiated with Kr, Ar and C ions are shown in Fig. 4. A detectable ion-induced increase of hardness is observed when fluence surpasses the 10^{10}, 5×10^{10} and 6×10^{11} ions/cm^2 limit for Kr, Ar and C ions correspondingly. The effect of hardening increases with fluence and approaches saturation at ~10^{15} ions/cm^2 at which the hardness by about a factor of two exceeds the hardness of a virgin crystal. The depth profiles of hardness in a great part of the ion range correlate with those of the electronic energy loss. An exception is the end-of-range region where high values of hardness at high fluences are maintained despite of the decrease of electronic energy loss to low values. The result allows us to conclude that a significant contribution in hardening here comes from the damage created by nuclear stopping mechanism.

We compared the dependence of ion-induced hardening on fluence for LiF: Ar samples (Fig. 4d) at two depth positions: (1) – at the Bragg's maximum (depth 4 μm), where the contribution of nuclear loss is negligible and damage is determined by electronic stopping mechanism, and (2) – close to the end-of-range (depth 11.7 μm), where the contribution of nuclear loss becomes dominant and the effect from electronic loss at moderate fluences (3×10^{11} ions/cm^2) becomes negligible (Fig. 4c). The results show that strong hardening at a correspondingly high fluence can be reached by both mechanisms (Fig. 4d). However, the hardening curve corresponding to the nuclear stopping is shifted by more than one order of magnitude towards higher fluences. Similar behavior – minor or negligible contribution of nuclear mechanism at low and moderate fluences and a remarkable increase of the effect at the highest fluences was observed also for Kr and C ions. We can conclude that the elastic collision (nuclear) mechanism is less effective for damage creation than the exciton mechanism.

The damage structures were revealed by selective chemical etching [14,15]. The results are shown in Fig. 5. Profile surfaces oriented normal to the irradiated surface were prepared by cleaving the irradiated sample (Fig. 5a) [16]. Fig. 5b is an AFM image showing a pattern of dislocation etch pits in the sample irradiated with ^{12}C ions at fluence

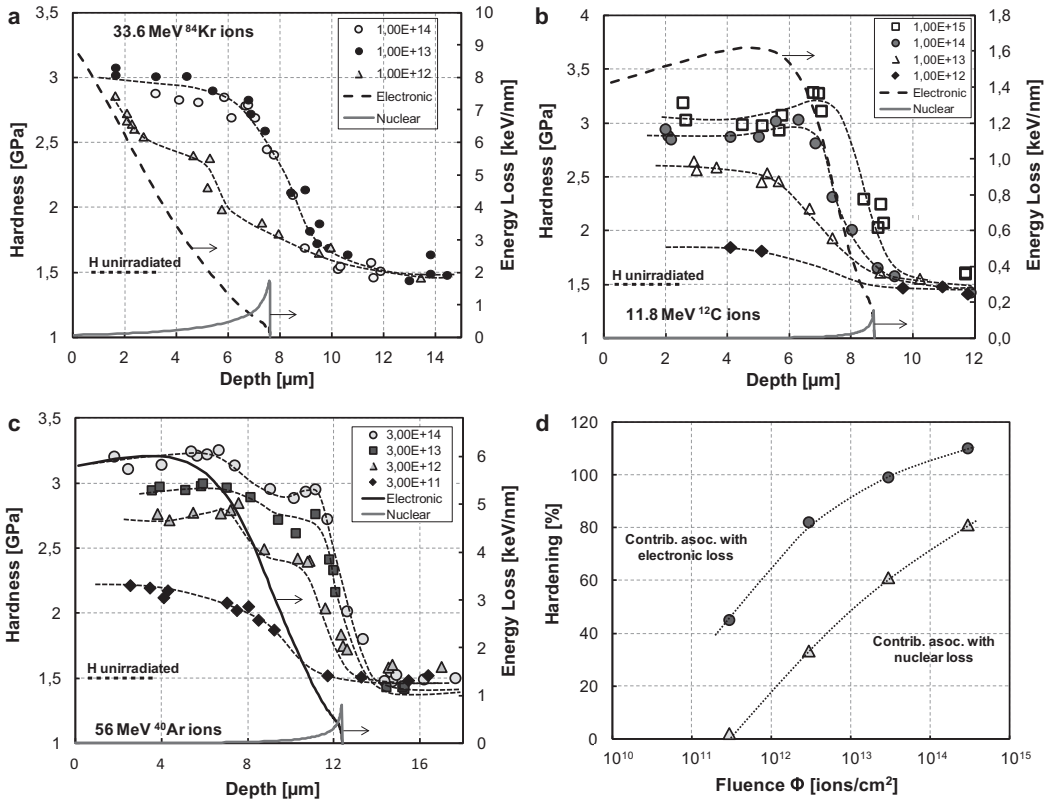

Fig. 4. Depth profiles of hardness in LiF crystals irradiated with (a) – ^{84}Kr ions, (b) – ^{12}C ions and (c) – ^{40}Ar ions; (d) – dependence of hardening on fluence for ^{40}Ar ions at the depth of 4 μm, where the ion stopping is determined by electronic energy loss, and at 11.7 μm depth where dominates nuclear energy loss.

of 10^{13} ions/cm^2 in which numerous square-based etch pits of different size are clearly seen. The evolution of dislocation structure along the ion path is strongly affected by the fluence. As shown for Kr ions, well-etchable dislocations at low fluences are formed in the beginning part of the ion path, where the highest values of electronic energy loss (4–8 keV/nm) are reached, while at a higher depth, where energy loss decreases to low values – rounded low contrast etch pits which belong to very small dislocation loops or their seeds are created (Fig. 5c). At high fluences, well recognizable dislocation etch pits for all ions are formed throughout the whole ion range. Their concentration increases and size decreases in the end-of-range region where a more intense formation of dislocation seeds is suggested due to contribution of nuclear loss mechanism (Fig. 5d).

There is a rather direct correlation between the shape of the ion induced dislocation etch pits and their size. When dislocation loop intersects the surface under investigation, it creates a mutually related pair of etch pits, the distance between which approximately characterizes the size of the loop. During chemical etching of small loops the

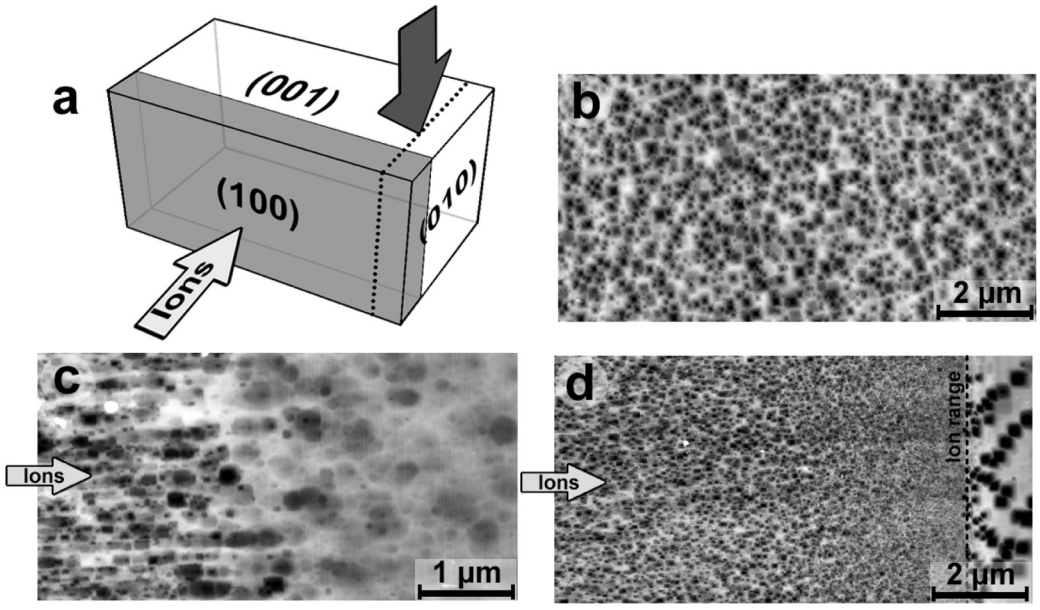

Fig. 5. (a) – scheme of sample preparation by cleaving of irradiated crystal. Cleavage plane is marked by a dashed line. Colored layer represents the irradiated zone.
(b) – etch pits of ion-induced dislocations on LiF surface, irradiated with ^{12}C ions at 10^{13} ions/cm^2; (c) – etch pits on profile surface irradiated with ^{84}Kr ions at 10^{12} ions/cm^2 and (d) – Dislocation pattern on etched profile surface irradiated with ^{40}Ar ions at 3×10^{14} ions/cm^2 (left side) and in the adjacent unirradiated zone beyond the range (right side). Direction of ion beam is shown by arrow and the end of ion range by a dashed line.

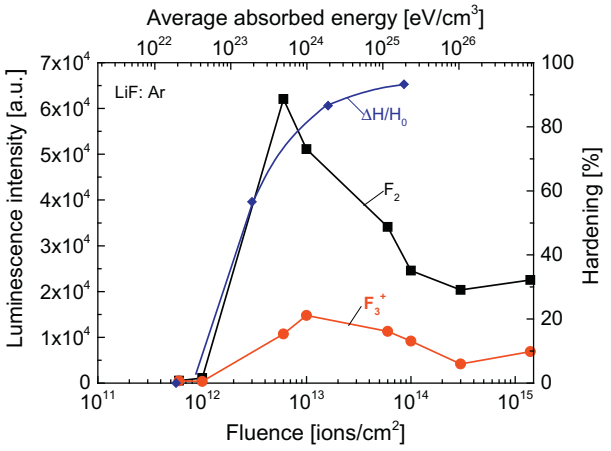

Fig. 6. Dose dependence of the hardening ($\Delta H/H_0$) and luminescence intensity of F_2 and F_3^+ centers in LiF irradiated with ^{40}Ar ions. Data from the profile curves (Figs. 3c,d and 4d) at a constant depth (11 μm).

pits might merge forming almost square shaped etch pits or elongated rectangles [5]. Such rectangular etch pits of dislocation loops at a higher magnification can be seen in Fig. 5c (left side) and Fig. 5d (left side). Rounded low-contrast etch pits like those shown in Fig. 5c (right side) can be ascribed to very small dislocation loops (around the lower limit for stable loops ~7–10 nm). Rough estimates based on AFM measurements of the etch pit length and width for Ar ions (Fig. 5d) give the size of dislocation loops in tens of nm (up ~60 nm). Concentration of these loops at high fluences exceeds 10^{10} cm^{-2}.

Another cause of the dislocation generation is long-range stresses due to volume expansion (swelling) of irradiated crystal, which arise at the vicinity of the interface between irradiated and unirradiated zones. At high fluences stresses in the adjacent unirradiated crystal as a softer medium can surpass the dislocation yield stress and create dislocation rows (slip lines) along the (110) planes inclinated at 45^0 to (001) face [17] as shown in Fig. 5d.

4. Discussion

Formation of dislocations as main extended defects created in LiF at room temperature irradiation with swift heavy ions is well established [4,5,18]. Ions with electronic energy loss < 10 keV/nm, used in the present study, create mainly small dislocation loops the maximum density of which at high fluences tends to exceed 10^{10} cm^{-2}. Accumulation of dislocations as strong obstacles for plastic deformation leads to a remarkable effect of ion induced hardening while point defects play a minor role [19]. Both, the formation of dislocations and hardening appear at an early stage of track overlapping [5,18].

Taking into account the high mobility of interstitials, mainly interstitial type dislocation loops can be formed. A perfect prismatic interstitial dislocation loop in ionic crystals requires aggregation of equal numbers of anion and cation interstitials. However, swift ions in alkali halides create damage by the exciton mechanism mainly in the anion sublattice, while the cation sublattice remains intact. Hobbs proposed a model in which the growth of dislocations occurs when di-halide molecule formed from H-centers occupies a lattice position and as a result expels an anion and a cation required for a perfect dislocation [20]. Such reaction becomes possible in the local stress field on edges of dislocation loops and other nano-scale defects [21]. Formation of dislocation seeds is observed already in individual ion tracks [5]. Intensive growth of dislocations and F-center aggregates is observed at the stage of track overlapping when ions hit pre-irradiated areas where new radiation defects are created as well as different structural transformations (aggregation or decomposition, growth or recombination, *etc.*) in the system of already existing defects can be activated [12,22].

The evolution of dislocation structure determines the hardening effect. At the highest fluences (about 10^{15} ions/cm^2) the hardness turns to saturation and approaches the upper limit for heavily irradiated LiF (3.5–4 GPa) due to a change in the mechanism of plastic deformation from homogenous dislocation glide to localized deformation in shear bands [23]). The irradiation dose at this fluence reaches 3 GGy for Kr ions, 2.7 GGy for Ar ions and 819 MGy for C ions.

Both, the electronic stopping and the nuclear stopping mechanisms are involved in the damage creation. The depth profiles of hardening show the highest effect around the Bragg's maximum of electronic energy loss. At high fluences, an additional maximum appears also in the tail part of the ion range due to the contribution of nuclear stopping mechanism.

The damage *via* electronic stopping occurs mainly in the anion sublattice while the damage by nuclear stopping is produced in both the anion and the cation sublattices. The latter causes formation of dislocations and hardening only in a narrow (width about 3 μm) end-of-range zone. A peculiarity of damage *via* nuclear stopping is the creation of anion and cation interstitials necessary for the formation of dislocation seeds that intensifies the nucleation of dislocations. As a result, dislocations revealed in the tail part of the ion path are smaller and their density is higher (Fig. 5d).

Considering possible mutual interaction between aggregate color centers and dislocations, the comparison of the dose dependence for ion-induced hardening and luminescence intensity from F_2 and F_3^+ centers at a constant depth (11 μm) was performed using the data for LiF: Ar samples (Fig. 6). The intensity of luminescence increases up to fluence of 6×10^{12} ions/cm^2 above which its quenching is clearly seen while the increase of hardening determined by the accumulation of extended defects continues and turns to saturation at a comparatively high concentration ($> 10^{10}$ cm^{-2}). It should be taken into account that dislocations in alkali halides and other materials serve as sinks and absorption sites for different radiation defects and impurities [15]. The stress field of dislocations could play an activating role in the interaction processes and reactions.

5. Conclusion

- The depth profiles of ion-induced damage in LiF have been studied using photoluminescence from F_2 and F_3^+ aggregate color centers, dislocation etching and nanoindentation.
- For LiF irradiated with 34 MeV ^{84}Kr, 56 MeV ^{40}Ar and 12 MeV ^{12}C ions, a notable contribution of nuclear loss in damage production and hardening has been observed. The effect dominates in the end-of-range region at fluences above 10^{13} ions/cm^2.
- Quenching of photoluminescence of F_2 and F_3^+ aggregate color centers at high irradiation fluences has been observed. The interaction of aggregate color centers with ion-induced dislocations, the stress field of which could suppress the luminescence, is suggested as one of the possible reasons.

Acknowledgements

I. Manika, J. Maniks and R. Zabels acknowledge the national project IMIS2. A. Dauletbekova, A. Akilbekov, M. Zdorovets and A. Seitbayev acknowledge the GF AP05134257of Ministry of Education and Science the Republic of Kazakhstan.

Reference

[1] K. Schwartz, C. Trautmann, T. Steckenreiter, O. Geiß, M. Krämer, Damage and track morphology in LiF crystals irradiated with GeV ions, Phys. Rev. B 58 (1998) 11232–11240.

[2] P. Thevenard, A. Perez, J. Davenas, C.H.S. Dupuy, Coloration of LiF by 56 MeV α-particles and 28 MeV deuterons. II. F_2^+ centre evolution, Phys. Status Solidi A 10 (1972) 67–72.

[3] M. Toulemonde, C. Trautmann, E. Balanzat, K. Hjort, A. Weidinger, Track formation

and fabrication of nanostructures with MeV-ion beams, Nucl. Instr. Meth. B 216 (2004) 1–8.
[4] J. Maniks, I. Manika, R. Zabels, R. Grants, E. Tamanis, K. Schwartz, Nanostructuring and strengthening of LiF crystals by swift heavy ions: AFM, XRD and na-noindentation study, Nucl. Instr. Meth. B 282 (2012) 81–84.
[5] R. Zabels, I. Manika, K. Schwartz, J. Maniks, R. Grants, MeV–GeV ion induced dislocation loops in LiF crystals, Nucl. Instr. Meth. B 326 (2014) 318–321.
[6] A. Perez, E. Balanzat, J. Dural, Experimental study of point defect creation in high-energy heavy-ion tracks, Phys. Rev. B 41 (1990) 3943–3950.
[7] V.A. Skuratov, Kim. Jong Gun, J. Stano, D.L. Zagorski, In situ luminescence as monitor of radiation damage underswift heavy ion irradiation, Nucl. Instr. Meth. B 245 (2006) 194–200.
[8] V.A. Skuratov, N.S. Kirilkin, Yu.S. Kovalev, T.S. Strukova, K. Havanscak, Depth-resolved photo- and ionoluminescence of LiF and Al_2O_3, Nucl. Instr. Meth. B 245 (2012) 194–200.
[9] W.C. Oliver, G.M. Pharr, An improved technique for determining hardness and elastic modulus using load and displacement sensing indentation experiments, J. Mater. Res. 7 (1992) 1564–1583.
[10] A. Russakova, M.V. Sorokin, K. Schwartz, A. Dauletbekova, A. Akilbekov, M. Baizhumanov, M. Zdorovets, M. Koloberdin, Color center accumulation in LiF crystals under irradiation with MeV ions: optical spectroscopy and modeling, Nucl. Inst. Methods Phys. Res. B 313 (2013) 21–25.
[11] G. Baldachini, F. Menchini, R.M. Montereali, Concentration quenching of the emission of F_3^+ and F_2 color centers in LiF, Radiat. Eff. Defects Solids 155 (2001) 71–75.
[12] V.A. Skuratov, S.M. Abu-AlAzm, V.A. Altynov, (1–3) MeV/amu heavy ion irradiation effects on optical properties of Al_2O_3, Mater. Sci. Forum 248–249 (1997) 399–403.
[13] H.P. Hirth, J. Lothe, Theory of Dislocations, Wiley, New York, 1982.
[14] J.J. Gilman, W.G. Johnston, Dislocations, point-defect clusters, and cavities in neutron irradiated LiF crystals, J. Appl. Phys. 29 (1958) 877–888.
[15] J.J. Gilman, W.G. Johnston, G.W. Sears, Dislocation etch pit formation in lithium fluoride, J. Appl. Phys. 29 (1958) 747–754.
[16] I. Manika, J. Maniks, K. Schwartz, C. Trautmann, Hardening and formation of dislocation structures in LiF crystals irradiated with MeV–GeV ions, Nucl. Instr. Meth. B 196 (2002) 299–307.
[17] I. Manika, J. Maniks, K. Schwartz, M. Toulemonde, C. Trautmann, Hardening and long-range stress formation in lithium fluoride induced by energetic ions, Nucl. Instr. Meth. B 209 (2003) 93–97.
[18] R. Zabels, I. Manika, K. Schwartz, J. Maniks, A. Dauletbekova, R. Grants, M. Baizhumanov, M. Zdorovets, Formation of dislocations and hardening of LiF under high-dose irradiation with 5–21 MeV ^{12}C ions, Appl. Phys. A 123 (2017) 1–8 art. Nr. 320.
[19] I. Manika, J. Maniks, K. Schwartz, Swift-ion-induced hardening and reduction of dislocation mobility in LiF crystal, J. Phys. D. Appl. Phys. 41 (2008) art. Nr. 074008.
[20] L.W. Hobbs, A.E. Hughes, D. Pooley, A study of interstitial clusters in irradiated alkali halides using direct electron microscopy, Proc. R. Soc. Lond. A332 (1973) 167–185.
[21] C.R.A. Catlow, K.M. Diller, L.W. Hobbs, Irradiation-induced defects in alkali halide crystals, Philos. Mag. A 42 (1980) 123–150.
[22] S.J. Zinkle, V.A. Skuratov, Track formation and dislocation loop interaction in spinel irradiated with swift heavy ions, Nucl. Instr. Meth. B 141 (1998) 737–746.
[23] J. Maniks, R. Zabels, I. Manika, Shear banding mechanism of plastic deformation in LiF irradiated with swift heavy ions, IOP Conf. Ser., Mater. Sci. Eng. 38 (2012) 012017.